

# Comparisons of Free-Flight and Wind-Tunnel Data on Slender Cones

JACK D. WHITFIELD\* AND B. J. GRIFFITH†  
 ARO, Inc., Arnold Air Force Station, Tenn.

### Nomenclature

- $C_H$  = heat-transfer coefficient
- $C_p$  = pressure coefficient
- $C_\infty$  = form of Chapman-Rubesin viscosity coefficient,  $\mu_w/\mu_\infty = C_\infty T_w/T_\infty$
- $C^*$  = form of Chapman-Rubesin viscosity coefficient (see Ref. 6)
- $d$  = nose diameter
- $K$  = nose drag coefficient
- $T$  = temperature
- $\alpha$  = angle of attack, rad
- $\gamma$  = ratio of specific heats
- $\epsilon = (\gamma - 1)/(\gamma + 1)$
- $\mu$  = gas viscosity
- $\psi$  = nose radius/base radius

### Subscripts

- $d$  = base on nose diameter
- $0$  = stagnation conditions
- $w$  = wall conditions
- $\infty$  = freestream conditions

THE role of the near-perfect gas hypersonic wind tunnel in the development of missiles and aircraft often has been hampered by questions of support interference and real-gas effects. The purpose of this note is to demonstrate by a comparison of data the apparent lack of support interference effects on forebody flow fields of slender cones and that so-called real-gas effects on the stability, drag, and heat-transfer rates for slender cones are insignificant at velocities up to 18,000 fps.

Figures 1 and 2 are correlations (following Whitfield and Wolny<sup>1</sup>) of the experimental normal force and pitching moment data on 8° and 9° half-angle ( $\theta_c$ ) slender cones from the

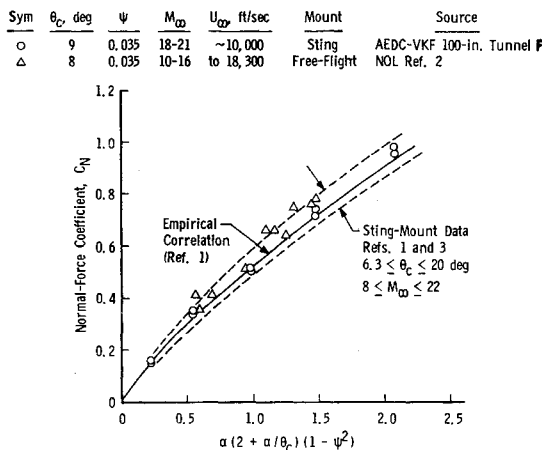


Fig. 1 Comparison of sting-mount and free-flight normal force data.

Received October 8, 1964. This work was sponsored by the Arnold Engineering Development Center (AEDC) Air Force Systems Command, U. S. Air Force, under Contract No. AF 40(600)-1000 with ARO, Inc., Operating Contractor, AEDC.

\* Manager, Hypervelocity Branch, von Kármán Gas Dynamics Facility. Associate Fellow Member AIAA.

† Supervisor, Aerodynamics Section, Hypervelocity Branch, von Kármán Gas Dynamics Facility. Associate Fellow Member AIAA.

Sym	$\theta_c$ , deg	$\psi$	$M_\infty$	$U_\infty$ , ft/sec	Mount	Source
○	9	0.035	18-21	~10,000	Sting	AEDC-VKF 100-in. Tunnel
△	8	0.035	10-16	to 18,300	Free-Flight	NOL Ref. 2

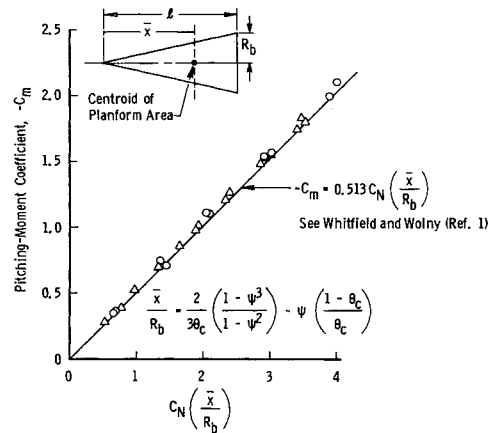


Fig. 2 Comparison of sting-mount and free-flight pitching-moment data.

Naval Ordnance Laboratory (NOL) aeroballistic range<sup>2</sup> and the AEDC-VKF 100-in. hypersonic Mach 20 tunnel (F), respectively. These data are relatively insensitive to Mach number  $M_\infty$  and Reynolds number  $Re$ , per se, and therefore they offer some assessment of real-gas and/or support interference effects. A comparison of the NOL and AEDC-VKF data indicates that the free-flight data at velocities ( $U_\infty$ ) up to 18,000 fps are in excellent agreement with the essentially perfect gas sting mounted wind-tunnel data. Also worthy of note is the fact that both sets of data agree with previously published data.<sup>1, 3</sup>

A summary of drag data from slender cones obtained with free-flight and balance techniques is shown in Fig. 3. The viscous drag coefficient  $\Delta C_{D_v}$  (total forebody drag less inviscid pressure drag) is plotted vs the hypersonic viscous parameter  $\bar{v}_\infty$ . Note that the cold-wall NOL-range data agree with previously published<sup>4</sup> high Mach number sting-mounted data. The AEDC-VKF free-flight data<sup>4</sup> ( $T_w/T_0 \approx 0.33$ ) were taken in the 50-in. Mach 10 tunnel by launching models from a pneumatic launch tube obtained through the courtesy of Bain Dayman (Jet Propulsion Laboratories). The agreement of the range free-flight data and the previous balance data and the consistent trend of the Mach 10 free-flight and balance data (with  $T_w/T_0$ ) certainly indicate no appreciable support interference or real-gas effects. Recent slender cone free-flight data published by Dayman<sup>5</sup> indicate greater viscous effects than the present data. No reason can be noted at present for the apparent discrepancy between the data reported by Dayman and the present data.

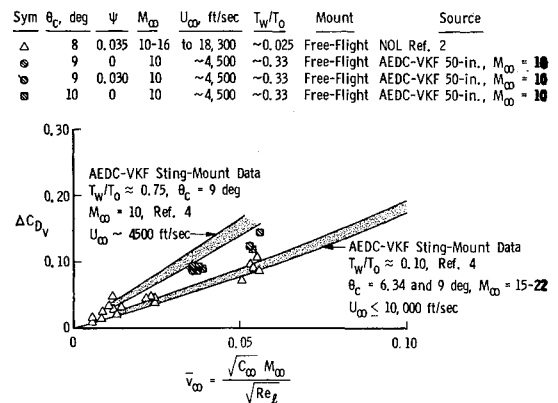


Fig. 3 Comparison of sting-mount and free-flight viscous drag data,  $\alpha = 0^\circ$ .

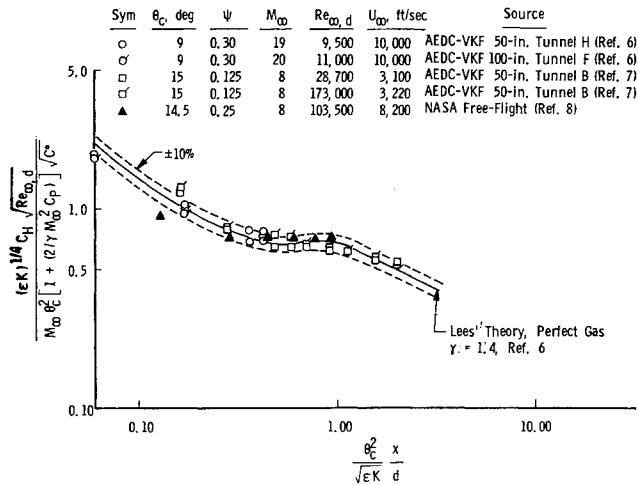


Fig. 4 Correlation of heat-transfer distribution to spherically blunted cones.

Figure 4 presents a correlation (following Griffith and Lewis<sup>6</sup>) of experimental and theoretical heat-transfer data over slender cones. The data presented represent data<sup>7</sup> from the AEDC-VKF 50-in. Mach 8 tunnel (B), data<sup>6</sup> from the AEDC-VKF 50- and 100-in. Mach 20 tunnels (H and F) and free-flight data<sup>8</sup> taken by NASA (NACA) personnel on the conical nose region of a spacecraft configuration. This correlation again indicates that support interference effects on the forebody are insignificant in the flight regime represented by these data.

In conclusion, the comparisons with free-flight data indicate that, for some situations of interest, real-gas effects are insignificant at velocities up to 18,000 fps and that support interference effects are negligible. Therefore, in this speed range it is possible to provide significant flight simulation in terms of Mach and Reynolds numbers alone, i.e., in existing test facilities that operate in the velocity regime of 10,000 fps.

#### References

- Whitfield, J. D. and Wolny, W., "Hypersonic static stability of blunt slender cones," Arnold Engineering Development Center TDR-62-166 (August 1962); also AIAA J. 1, 486 (1963).
- Lyons, W. C., Jr. and Brady, J. J., "Hypersonic drag, stability, and wake data for cones and spheres," AIAA J. 2, 1948-1956 (1964).
- Edenfield, E. E., "Comparison of hotshot tunnel force, pressure, heat-transfer and shock shape data with shock tunnel data," Arnold Engineering Development Center TDR-64-1 (January 1964).
- Whitfield, J. D. and Griffith, B. J., "Hypersonic viscous drag effects on blunt slender cones," AIAA J. 2, 1714-1722 (1964).
- Dayman, B., Jr., "Free-flight hypersonic viscous effects on slender cones," AIAA Preprint 64-46 (January 1964); also AIAA J. (submitted for publication).
- Griffith, B. J. and Lewis, C. H., "Laminar heat transfer to spherically blunted cones at hypersonic conditions," AIAA J. 2, 438-444 (1964).
- Rhudy, J. P., Hiers, R. S., and Rippey, J. O., "Investigation of hypersonic flow over blunted plates and cone," Arnold Engineering Development Center TN-60-93 (May 1960).
- Bland, W. M., Jr., Rumsey, C. B., Lee, D. B., and Kolenkiewicz, R., "Free-flight aerodynamic-heating data to a Mach number of 15.5 on a blunted conical nose with a total angle of 29°," NACA RML57F28 (August 1957).

## Reduction of Stiffness and Mass Matrices

ROBERT J. GUYAN\*

North American Aviation, Inc., Downey, Calif.

JUST as it is often necessary to reduce the size of the stiffness matrix in static structural analysis, the simultaneous reduction of the nondiagonal mass matrix for natural mode analysis may also be required. The basis for one such reduction technique may follow the procedure used in Ref. 1 for the stiffness matrix, namely, the elimination of coordinates at which no forces are applied.

Arrange the structural equations  $\{F\} = [K]\{x\}$  so that after partitioning in the form

$$\begin{Bmatrix} F_1 \\ F_2 \end{Bmatrix} = \begin{bmatrix} A & B \\ B' & C \end{bmatrix} \begin{Bmatrix} x_1 \\ x_2 \end{Bmatrix}$$

the forces  $F_2$  are to be zero. The two resulting equations yield

$$F_1 = (A - BC^{-1}B')x_1$$

from which the reduced stiffness matrix is seen to be

$$K_1 = A - BC^{-1}B'$$

The foregoing amounts to a coordinate transformation  $x = Tx_1$  or

$$\begin{Bmatrix} x_1 \\ x_2 \end{Bmatrix} = \begin{bmatrix} I \\ -C^{-1}B' \end{bmatrix} \{x_1\}$$

If the structure energies are written  $T = \frac{1}{2}\dot{x}'M\dot{x}$  and  $V = \frac{1}{2}x'Kx$  and the foregoing transformation is employed, the result is

$$T = \frac{1}{2}\dot{x}_1'T'MT\dot{x}_1$$

$$V = \frac{1}{2}x_1'T'KTx_1$$

The reduced stiffness matrix is seen to be  $K_1 = T'KT$  and the reduced mass matrix  $M_1 = T'MT$ . Then with

$$[M] = \begin{bmatrix} \bar{A} & \bar{B} \\ \bar{B}' & \bar{C} \end{bmatrix}$$

the reduced mass matrix becomes

$$M_1 = \bar{A} - \bar{B}C^{-1}B' - (C^{-1}B')'(\bar{B}' - \bar{C}C^{-1}B')$$

In the case of the reduced stiffness matrix, none of the structural complexity is lost since all elements of the original stiffness matrix contribute. However, in the reduced mass matrix, combinations of stiffness and mass elements appear. The result is that the eigenvalue-eigenvector problem is closely but not exactly preserved. Some comparative results are reported in Ref. 2 for beam vibrations.

#### References

- Turner, M. J., Clough, R. W., Martin, H. C., and Topp, L. J., "Stiffness and deflection analysis of complex structures," J. Aeronaut. Sci. 23, 805-823 (1956).
- Archer, J. S., "Consistent mass matrix for distributed mass systems," Proc. Am. Soc. Civil Engrs. 89, 161-178 (August 1963).

Received September 8, 1964.

\* Research Specialist, Space and Information Systems Division. Member AIAA.